International Journal of
Turbomachinery
Propulsion and Power

MDPI

Article

Heat Load Development and Heat Map Sensitivity Analysis for Civil Aero-Engines

Alireza Ebrahimi *, Soheil Jafari and Theoklis Nikolaidis

Centre for Propulsion and Thermal Power Engineering, School of Aerospace, Transport and Manufacturing, Cranfield University, Bedford MK43 0AL, UK
* Correspondence: alireza.ebrahimi@cranfield.ac.uk

Abstract: The design complexity of the new generation of civil aero-engines results in higher demands on engines' components, higher component temperatures, higher heat generation, and, finally, critical thermal management issues. This paper will propose a methodological approach to creating physics-based models for heat loads developed by sources, as well as a systematic sensitivity analysis to identify the effects of design parameters on the thermal behavior of civil aero-engines. The ranges and levels of heat loads generated by heat sources (e.g., accessory gearbox, bearing, pumps, etc.) and the heat absorption capacity of heat sinks (e.g., engine fuel, oil, and air) are discussed systematically. The practical research challenges for thermal management system design and development for the new and next generation of turbofan engines will then be addressed through a sensitivity analysis of the heat load values as well as the heat sink flow rates. The potential solutions for thermal performance enhancements of propulsion systems will be proposed and discussed accordingly.

Keywords: thermal management system; heat loads; aero-engines

Citation: Ebrahimi, A.; Jafari, S.; Nikolaidis, T. Heat Load Development and Heat Map Sensitivity Analysis for Civil Aero-Engines. *Int. J. Turbomach. Propuls. Power* **2024**, *9*, 25. https://doi.org/10.3390/ijtpp9030025

Academic Editors: Ralf Obertacke, Pete Loftus, Hanspeter Zinn and Björn Karlsson

Received: 14 March 2024
Revised: 22 May 2024
Accepted: 10 June 2024
Published: 2 July 2024

1. Introduction

Thermal Management Systems (TMSs) are crucial for enhancing the performance of aircraft engines by managing the excess heat loads generated by various components (e.g., bearings, gearboxes, pumps, generators, etc.) at different flight phases [1]. The primary goal of the TMS is to transfer excess heat to aircraft heat sinks (e.g., fuel, oil, and air) and utilize this energy to enhance the efficiency of the propulsion system and the aircraft. Moreover, the TMS aims to regulate the surface temperature of propulsion system components to prevent overheating, which can adversely affect their performance. This is particularly crucial for components like the power gearbox (PGB) in geared turbofan engines, the Accessory Gearbox (AGB), and electrical components in More Electric Aircraft (MEA) [2]. With respect to the very tight regulations set in the net zero 2050 strategy and Flight Path 2050 [3,4], along with increasing values of heat loads in new generations of aircraft engines [5], the optimal design of the thermal management system is crucial to enhance the performance of the propulsion system and reduce the aircraft's emission levels. A typical architecture of a TMS for an aero-engine is shown in Figure 1. As depicted in this figure, the engine oil, air, and fuel systems are integral parts of the TMS and should be optimally designed and integrated. The lubrication oil is normally used as the coolant in the components to absorb the generated heat. The hot oil then passes through heat exchangers, such as the Fuel Oil Heat Exchanger (FOHE) and the Air Oil Heat Exchanger (AOHE), to transfer the absorbed heat to engine fuel or air. The fuel system is designed to act as a heat sink for the oil system, cooling the oil and warming the fuel [6]. It is worth mentioning that the fuel at a higher temperature will enhance the fuel consumption of the engine [7]. However, if the fuel does not have enough capacity to take all the absorbed heat (due to certification limitations or operating temperature limits), the engine bypass and/or ram air could be used as another heat sink. The level of the oil flow rate, the order of lubricating the

components, and the architecture of the thermal management system will strongly depend on the thermal load values and available heat sinks at different flight phases.

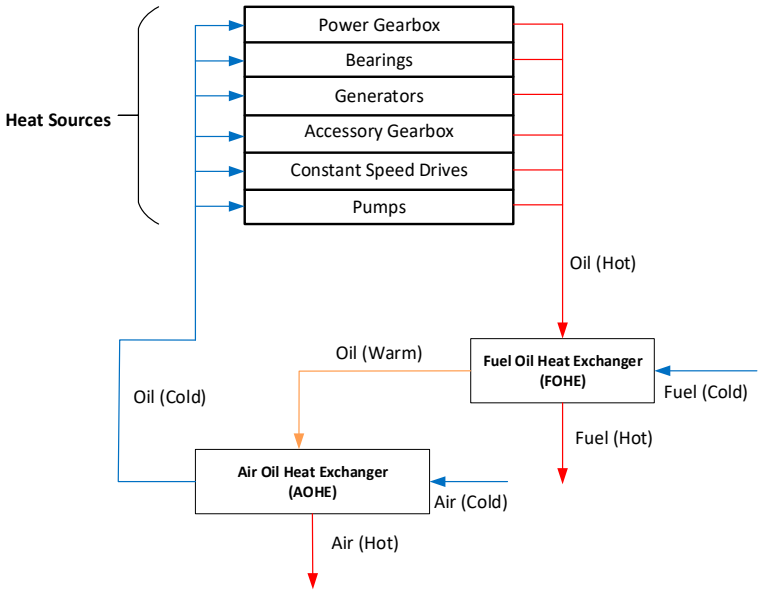

Figure 1. A conventional TMS architecture for aircraft applications (adapted from [6]).

In summary, the TMS should cope with three main challenges, including the component surface temperature, the temperature of the working fluid, and increasing thermal load values in new and next-generation propulsion systems [6]. The consequences of these issues will negatively affect the aircraft's fuel consumption and emission level due to its sensitivity to weight, ram, and/or external aerodynamic drag caused by installing cooling systems [5]. Figure 2 shows the thermal loads for different aircraft over time. The larger the air vehicle, the more variety of heat sinks are required for dealing with the thermal loads generated in the aircraft.

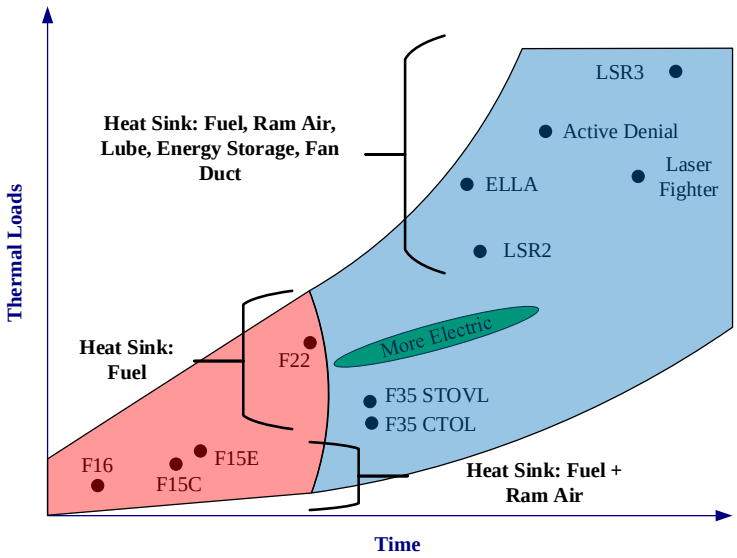

Figure 2. Thermal loads over time (adapted from [8]).

It should be noted that although the above figure primarily illustrates the heat loads over time for military engines, this trend is also applicable to civil aero-engines due to the rising integration of electrically powered subsystems, the upcoming introduction of ultra-high bypass geared turbofan engines, and the potential emergence of electrified propulsion.

These advancements are anticipated to result in substantial increases in onboard waste heat loads [2,5,9,10].

A more comprehensive literature review has shown that more than 1400 documents were published from 1964 that were completely or partially related to aircraft TMS study. It is evident that there is a significant increase in research interest in TMS, driven by the rising power demand and thermal loads of aero-engines. This trend underscores the growing importance of this topic (Figure 3). Almost 65% of the publications were conference papers, and the rest were either journals or technical reports. This involves the introduction of an integrated fuel thermal management system (combined airframe and engine) in [11] to different TMS architectures with cryogenic fuels (e.g., hydrogen) in [12].

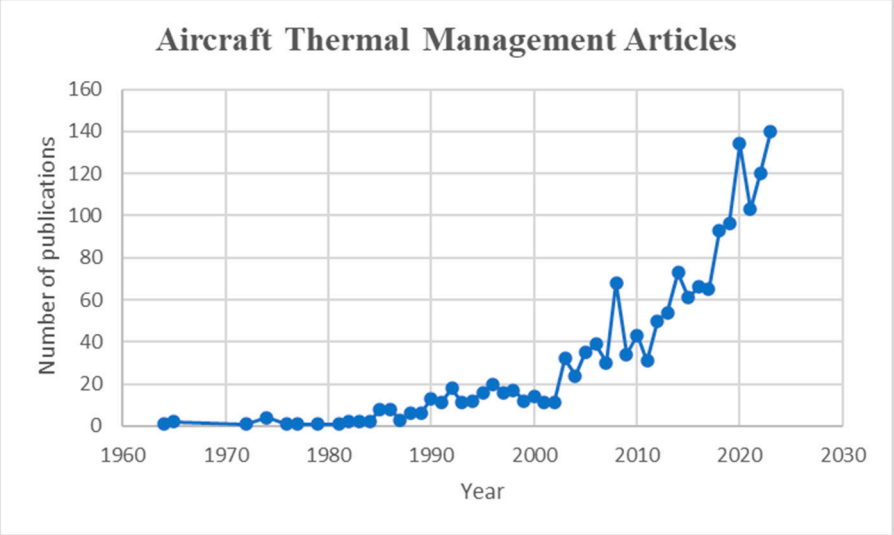

Figure 3. Publication distribution over time regarding aircraft TMSs (obtained from Scopus [13]).

In general, based on Pal and Severson [14], the TMS procedure includes five steps, which are heat loads developed in heat sources, heat acquisitions, thermal transport, heat rejection, and heat absorption in the terminal heat sink. Heat sources can be systems or components that generate excess heat either as a by-product of their function (such as energy-inefficient systems) or as their primary function (like cabin heaters) that need to be managed [5]. Heat acquisition will take place in the heat source components to transfer the excess heat to the coolant (e.g., oil). The use of local cooling may only sometimes be feasible in some cases, and waste heat must be transported over longer distances to heat sinks, so this is where thermal transport mechanisms are required. Heat rejection mechanisms work in a similar manner to heat acquisition mechanisms, or on the reverse principle. Finally, the terminal heat sinks refer to the destination of the thermal energy (e.g., fuel and air). In aircraft, fuel is an important heat sink since there is usually a large supply available that can be transported from one part of the aircraft to another. Preheating fuel before inserting it into the combustion chamber also has a thermodynamic advantage in enhancing the thermal efficiency of the engine [7,12,15]; however, the use of fuel as a heat sink is not without its risks and limitations, such as its flammability and tendency to coke when heated above certain temperatures [1,16].

Therefore, it is important to have an accurate vision of the values and levels of heat loads to develop the propulsion system heat map. This heat map will be used as an input in the thermal management system's design procedure. This paper presents and classifies heat load values generated by heat sources at different classes of turbofan engines. A preliminary sensitivity analysis is also carried out to illustrate the trend of technology in TMS design for new and next-generation propulsion systems.

2. Methodology and Approach

This section outlines the methodology and approach employed in this study. First, an overview of the heat sinks and heat sources in a standard civil aero-engine is provided. Next, the modeling process used to calculate power losses in various components is presented. Following this, TMS models based on thermal load equations are created and integrated with the engine model, which is developed in the MATLAB/Simulink environment. Finally, the sensitivity analysis of heat sinks in the engine model is performed. The methodology is presented in Figure 4 below.

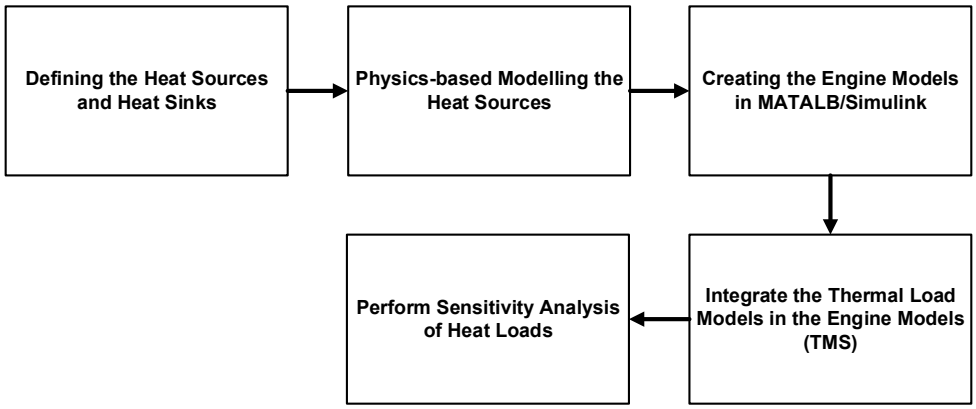

Figure 4. The paper methodology workflow.

2.1. Aero-Engine Heat Sources and Sinks

The thermal management system in gas turbine aero-engines is meticulously designed to efficiently handle the thermal loads generated during operation. It utilizes coolants to effectively transfer the thermal loads to heat sinks and distribute the thermal loads based on their capacity at various flight phases. The specific design of the system is contingent upon factors such as the number of heat sources, the thermal loads experienced during different flight phases, the properties of the coolant, the size and capability of the heat sink, the overall architecture of the thermal management system, and the type of cooling mechanism employed. The typical heat sources, sinks, and coolants used in aero-engines are listed in Table 1.

Table 1. Heat sources, heat sinks, and coolants used in aero-engines.

Heat Sources	Coolant	Heat Sinks
• Bearings (engine shaft bearings); • Accessory gearbox; • Pumps (fuel pump, oil pump, etc.); • Power gearbox (in geared turbofan engines).	• Engine oil; • Thermally neutral heat transfer fluids (TNHTFs).	• Engine fuel; • Air.

The process of designing and simulating an aero-engine thermal management system could begin with creating a physics-based model of engine heat sources. This involves developing a mathematical thermal model for engine bearings, gearboxes, pumps, etc., to calculate the thermal loads generated by each source under different operating conditions. There is in-house developed software available at Cranfield University for this purpose [17–19], and a brief description of the models, how they can be developed and validated, and the related pseudocodes and equations are provided in the below section.

2.2. Modeling Procedure

The Accessory Gearbox (AGB) drives the engine's accessories, like the generator, fuel and oil pumps, and hydraulic pumps. As a result, it is an essential element for the operation

of the engine or the aircraft on which it is mounted. The power loss mechanisms inside the gearbox can be separated into two groups: non-load-dependent losses and load-dependent losses. Non-load-dependent losses include churning losses caused by gears, seals, and bearings, and load-dependent losses are frictional losses caused by gears and bearings [20]. The power gearbox (PGB) is a reduction gearbox between the fan and the low-pressure (LP) shaft, allowing the latter to run at a higher rotational speed, thus enabling fewer stages to be used in both the LP turbine and the LP compressor, increasing efficiency and reducing weight. In the context of the PGB, load-dependent losses include bearing friction loss and gear mesh loss. Mechanical losses are generated by friction between mating gear teeth. There are three types of load-independent losses: bearing churning losses, gear windage losses, and oil seal losses. In comparison with other heat-producing mechanisms, the latter is usually ignored since its contribution is very small. Fluid dynamic effects, bearing viscous losses, and trapped fluid between gear teeth all contribute to these losses [17]. In summary, the total power loss can be the sum of non-load-dependent and load-dependent losses, as shown in the following equation:

$$P_{Total} = P_{Load_{dependent}} + P_{Non\text{-}load_{dependent}} \quad (1)$$

The complete explanation of the required equations for AGBs and PGBs was detailed in previous works [17–19], so in order to avoid repetition, these equations are presented in Figures 5 and 6, respectively.

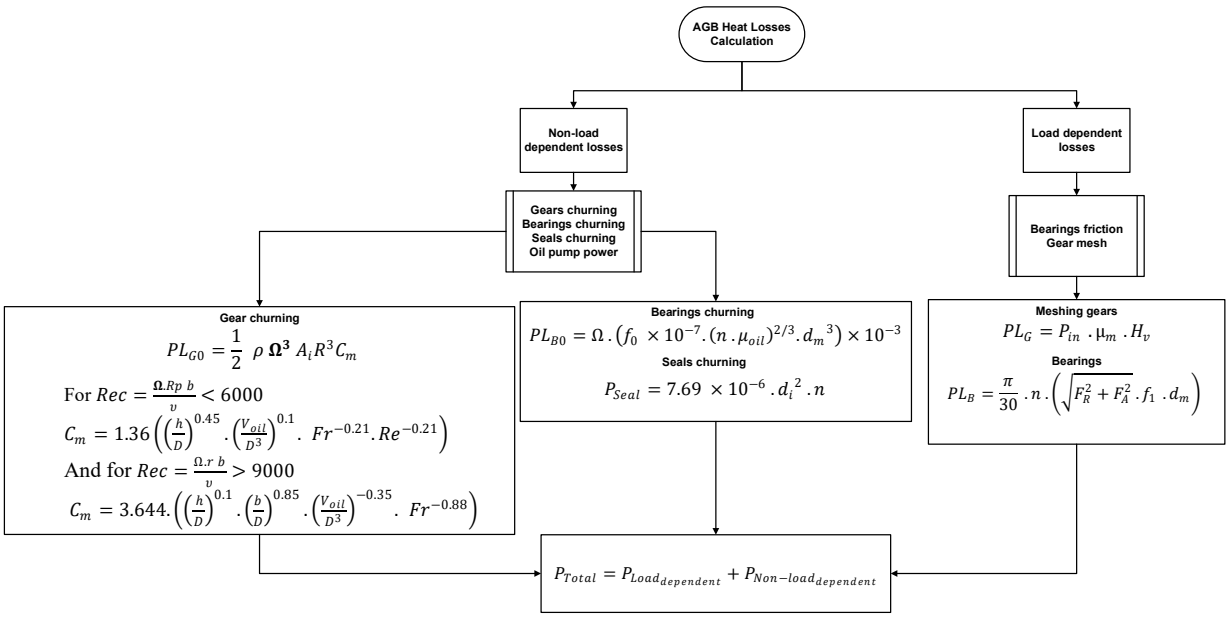

Figure 5. AGB heat loss calculation.

The heat loads generated in bearings are friction losses caused by several types of movements, such as sliding and rolling and drag between the lubricant and rolling elements [21,22]. Sliding friction losses occur primarily at low speeds due to microslips between surfaces during rolling motions, while rolling friction losses are caused by deformation effects and elastic hysteresis. Other heat loss mechanisms, including drag friction and seal friction, are normally generated when the lubricant acts as a friction force against the direction rolling elements and by the heat generated between the contact surfaces between the seal rubber and shaft, respectively. To calculate the heat loads in the bearings, a physics-based simulation program needed to be developed based on analyti-

cal/mathematical models. SKF proposed that by having the value of the friction moment, the total heat load generated in a bearing could be estimated as follows [23,24]:

$$Q = 0.105 \times 10^{-6} M\, n \tag{2}$$

where Q is the thermal load in kW; M is the friction moment in N · mm; and n is the shaft rotational speed in min^{-1}. This is a very straightforward method, as a gas turbine engine simulation program could calculate the rotational speed in each flight phase. So, the problem is just calculating the friction moment in the bearing. A critical literature review of the available modeling techniques showed different friction moment calculation methodologies. Three main methods are simplified approaches, load-based approaches, and correlation-based approaches. The most famous method in each category is presented in Table 2.

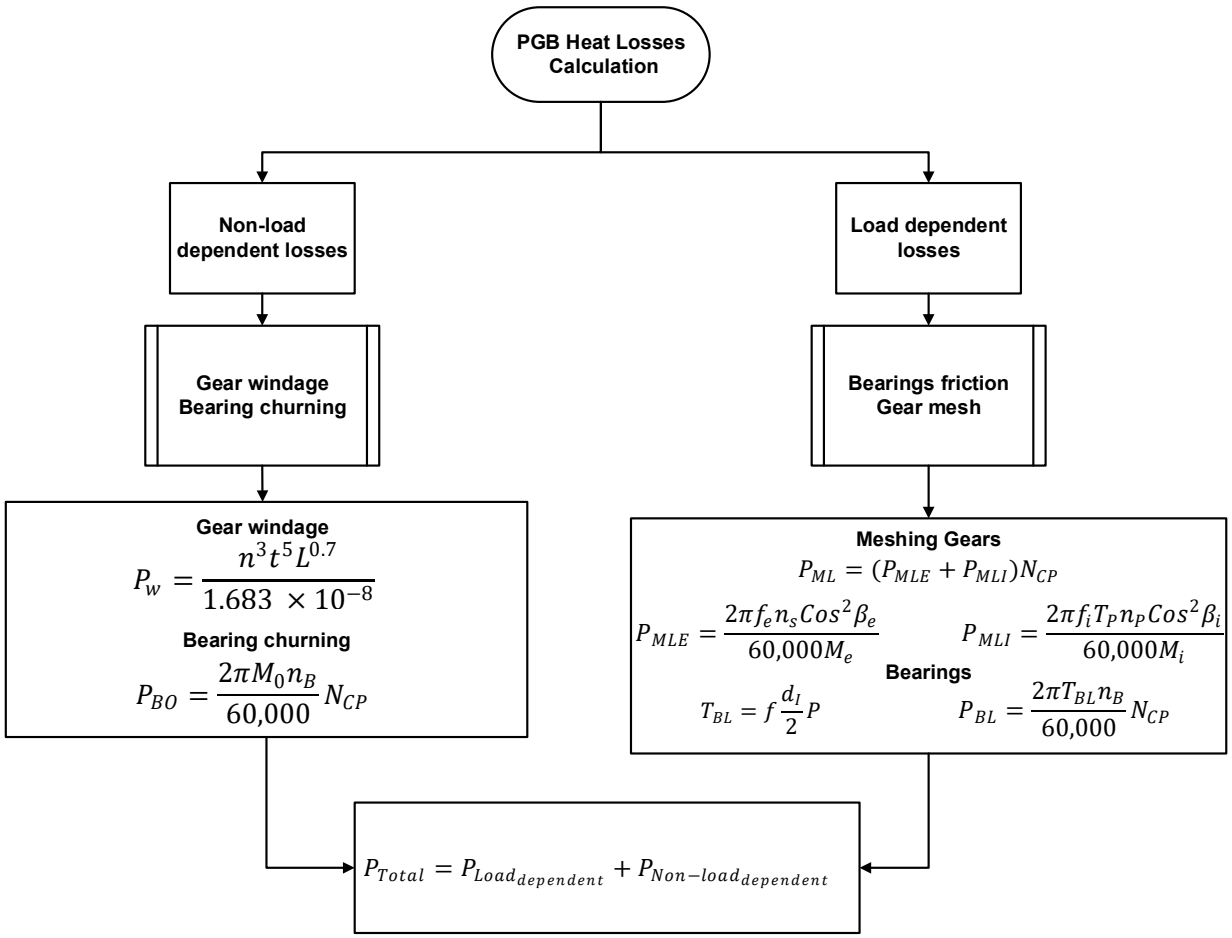

Figure 6. PGB heat loss calculation.

Table 2. Methods for calculating bearing friction moments.

Method	Formulation		Reference
I	$\mu = \frac{2M}{Pd}$	(3)	[23]
II	$M = M_0 + M_1$ $M_0 = 10^{-7} \times f_0 (\vartheta n)^{\frac{2}{3}} d_m^3$ $M_1 = f_1 P_1 d_m$	(4)	[22]
III	$M = 0.0264 \omega (D_1 + D_2)^2 + 3.24 \times 10^{-5} W^{1.5}$	(5)	[25]

SKF proposed the first method as a simplified technique to calculate the friction moment in bearings. In this method, μ is the friction coefficient typically selected from publicly available tables (based on the bearing type), P is the bearing load in N, and d is the bearing bore diameter in mm. Therefore, the heat loads generated in each bearing can be calculated by utilizing Equations (2) and (3), along with an engine performance simulation program.

The second method is one of the most precise methods in friction moment calculation. In this approach, the friction moment is divided into two main parts: load-dependent and non-load-dependent parts. The non-load-dependent part (M_0) is a function of f_0, which is the index for bearing type and lubrication type, ϑ, which is the operating viscosity in (mm^2/s), n, which is the bearing speed (rpm), and dm, which is the pitch circle diameter ($(D + d)/2$). The load-dependent part (M_1) is caused by the bearing load (P_1). In this equation, f_1 represents the index for bearing type and lubrication type. In this method, f_0 and f_1 are chosen based on the bearing type and can be found in publicly available tables (e.g., references [23,26]).

The third method is a correlation-based strategy. Dr. Styri of SKF proposed it based on his ball-bearing loss measurements. In this method, ω is the bearing width (inch); D_1 is the bore diameter (inch); D_2 is the outside diameter (inch); and W is the equivalent total load (lb). The literature and experimental validations from researchers in the field consistently support the conclusion that the second method is more accurate and better represents the actual heat loads generated by aero-engine bearings. Additionally, this method offers the advantage of modularity, dividing the friction moment into load-dependent and non-load-dependent parts. This allows for a more precise estimation of heat load at various flight phases based on the bearing loads, providing valuable insights for designers. Moreover, there are several reliable references for f_0 and f_1 that cover different types of bearings. This method could also be used in other applications where the bearing types are similar to aero-engines (e.g., maritime and land-based gas turbines). Therefore, method II was selected for developing the simulation program in this paper. Figure 7 illustrates the summary of three methods for bearing heat loss calculation.

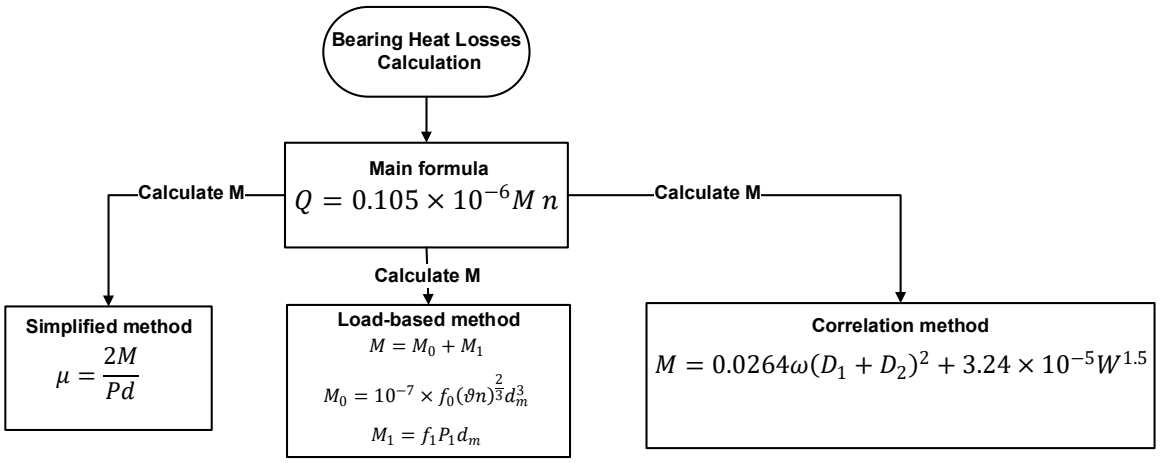

Figure 7. Bearing heat loss calculation.

3. Results

The research results indicate that engine size (maximum thrust) has the most significant impact on thermal load values, making it the primary parameter in the thermal management system design process. To illustrate this effect, Table 3 lists typical heat load values generated at take-off conditions for various sizes of civil turbofan engines. Three case studies have been selected for this purpose:

- The first case is a CFM-56 size engine with a take-off thrust of 18 klbf (80 kN). The simulation results obtained by Cranfield's in-house developed toolbox show that

53 kW of heat load should be transferred to the engine oil at take-off condition, including 18 kW from the accessory gearbox, 23 kW from the engine shaft bearings, and another 12 kW from the engine pumps, seals, etc. The validity of the results is verified through the MTU paper, which validated the heat loads of different components with experimental data (Figure 3 in reference [27]).

- The second case study demonstrated that increasing the engine size from a conventional turbofan to a geared turbofan, such as the PW1100G with a take-off thrust of 112 kN (25 klbf), dramatically increases the total heat to oil. The physics-based model developed for this engine's TMS system showed that the power gearbox is the primary source of heat loads in geared turbofan engines. Despite the high efficiency of planetary gearboxes (above 97%), significant heat is generated due to the large amount of power transferred by this component [17].
- For the third case study, one version of the UltraFan engine, an Ultra-High Bypass Turbofan with a take-off thrust of 280 kN, is simulated. The results showed that even with state-of-the-art PGB technology boasting over 99% efficiency, 592 kW of heat load is generated during take-off (the engine's low-pressure shaft power is around 64 MW [28]). Additionally, the heat load values in the bearings and accessory gearbox increase proportionally to the engine's thrust.

Table 3. Heat loads generated at take-off condition in different sizes of turbofan engines.

Case Study	Take-Off Thrust (klbf)	Bearing's Heat Load (kW)	AGB (kW)	PGB (kW)	Pumps, Seals, etc. (kW)	Total Heat (kW)
CFM56 size	18	23	18	-	12	53
PW1100G size	25	31	26	223	17	297
UltraFan size	63	55	53	592	23	722

3.1. Sensitivity Analysis of Heat Sources

An interesting result has been obtained from analyzing the heat loads at different case studies through a preliminary sensitivity check, as illustrated in Figure 8. The thrust (in klbf) and the heat loads produced by bearings, AGBs, and accessories (in kW) seem to be linearly related and correlated. However, it is evident that the effect of the AGB on heat loss generation increases with thrust. This should be considered in future high-power engine design procedures. Moreover, while the results from the physics-based models for accessories did not show a strong sensitivity to thrust, this can be explained by the fact that the load on accessories typically does not change significantly. Although more real data and case studies are needed to reinforce these conclusions, some quick remarks can be listed as follows:

- Overall, increasing the thrust leads to higher heat loads.
- In low thrust values, the level of thrust (in klbf) is well correlated with the value of AGB heat load (case studies 1 and 2).
- By increasing the thrust value, the correlation is more obvious with the bearing heat loads rather than those of the accessories.
- The slope of the bearing heat load values is slightly higher than those of the AGB in the low thrust ranges. However, at higher thrust levels, the slope for AGBs is higher than that of the bearing heat load.
- The thermal management system architecture design procedure is more sensitive to bearings and AGB characteristics than to accessories characteristics. This should be taken into account in the TMS design and development steps as well as in the definition of degradation management strategies.
- As a rule of thumb, a linear relationship could be fitted to the values of heat loads generated in bearings and the accessory gearbox as a function of thrust value. A more accurate curve-fitting procedure could be carried out by adding more case studies and experimental data.

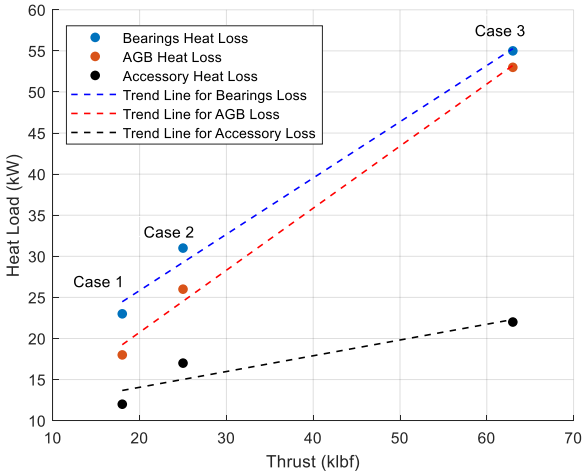

Figure 8. Heat loads of different components vs. engine thrust.

Another important aspect of the TMS that requires discussion is the variation in PGB mechanical efficiency throughout the flight mission. Although PGBs typically achieve high efficiency (over 95% in modern engines), the heat loss remains significant due to the substantial amount of power transferred by this component. Figure 9 shows PGB heat loss at different flight phases for the third case study. The heat load generated in the PGB is a function of many parameters, including low-pressure shaft power, rotational speed, geometry, oil characteristics, and material. Based on the physics-based equations, the most important parameters in this regard are the shaft power and the rotational speed [29]. As a result, the maximum heat load is generated at take-off and the beginning of the climb.

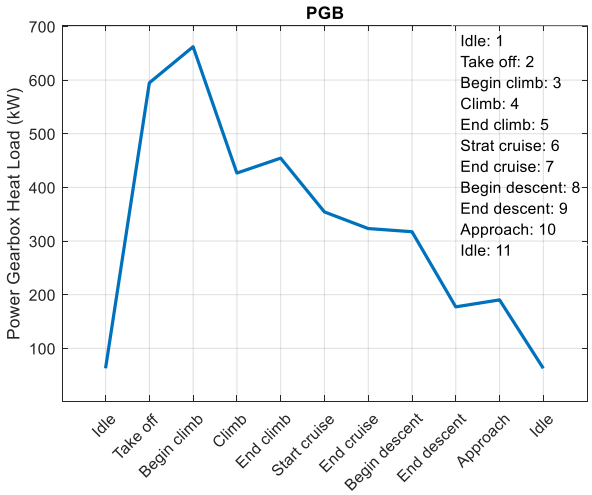

Figure 9. PGB heat loss during flight.

Figure 10 shows the variation of mechanical efficiency in the PGB at different flight phases. It should be noted that the efficiency is being changed at each flight phase (the results are coming from the physics-based model presented in [17]). However, except during idle conditions, this value consistently remains above 97%. Therefore, a useful guideline is that the heat load generated by the PGB in geared turbofans can be constrained as follows:

$$Q_{PGB} \leq 0.03 \times P_{LP\ shaft} \tag{6}$$

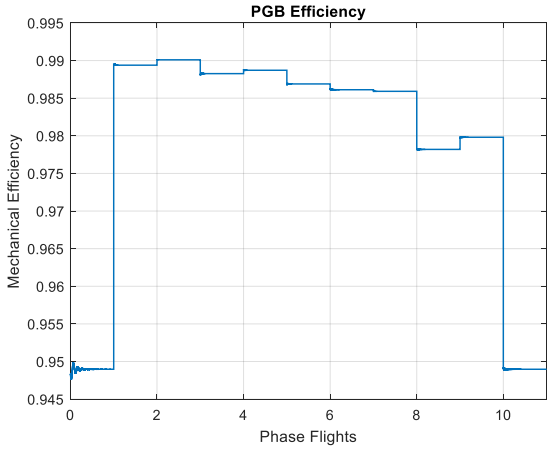

Figure 10. PGB mechanical efficiencies during flight.

3.2. Sensitivity Analysis of Heat Sinks

After discussing the heat sources and their values, an initial study was conducted to determine the effects of oil mass flow on PGBs, AGBs, and bearing exit oil temperature. Two scenarios have been defined and simulated in this regard:

- **Scenario I:** Increase/decrease the oil mass flow rate in all components (changing the size of the oil pump and the oil tanks accordingly).
- **Scenario II:** Changing the distribution of the oil flow rate in the components (in this scenario, the size of the oil pump and other TMS components is fixed, but the characteristics of the 3-way valve that distributes the oil flow rate to the bearing, AGB, and PGB compartments will be changed).

Figure 11 shows the result of scenario I. Decreasing the oil mass flow rate impacts the surface temperature and performance of all components, with the PGB being the most sensitive. This highlights the need for a precise health monitoring system for PGB lubrication in geared turbofan engines. While increasing the oil flow rate can reduce the compartment temperature, it requires a larger oil tank and a heavier thermal management system. This may be impractical from a design and manufacturing perspective and could negatively affect the overall propulsion system performance due to the additional weight.

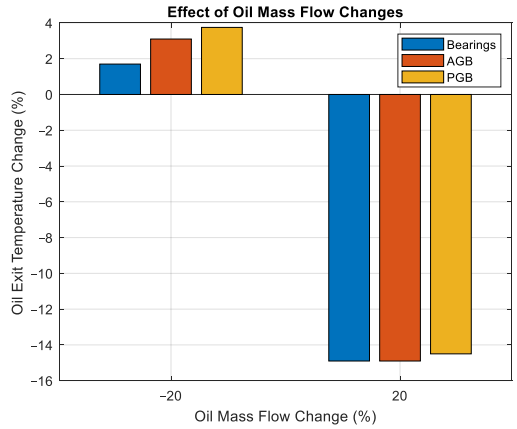

Figure 11. The effect of the oil mass flow rate on the exit temperature (scenario I).

Furthermore, Figure 12 presents the results of scenario II, in which, in one set of results, 90% of the oil flow rate will go through the PGB, 5% to the AGB, and 5% to the bearings. In another set of results, 70% of the oil will be circulated in the PGB, and 15% for the bearings and AGB will be used. The results indicate that the temperatures at the AGB exit oil are more influenced by distribution differences than other exit oil temperatures. This suggests that the design of the bearings and PGB is approaching an

optimal configuration, where variations in the oil flow rate will not significantly impact the exit oil temperature. According to [30,31], for the engine components, there is an optimum design point where oil mass flow should not significantly affect the exit temperature of the heat sources. Consequently, the optimal design of AGBs for turbofan engines could be a very challenging topic for future research studies.

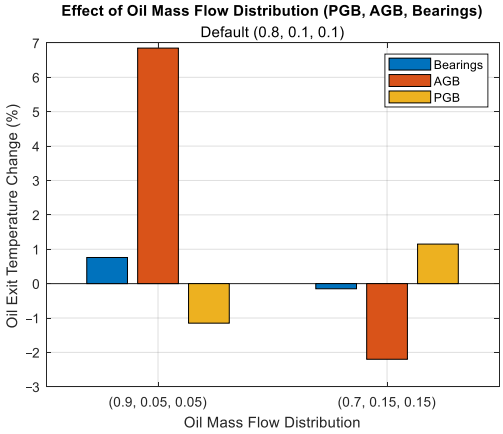

Figure 12. The effect of oil mass flow distribution on the exit temperature (scenario II).

4. Conclusions

This paper presents a methodological approach to analyzing the behavior of heat sources and heat sinks in the thermal management of propulsion systems. A set of physics-based models for simulating heat sinks is introduced. Three civil engines with different thrust values—a high-bypass turbofan, a geared turbofan, and an ultra-high bypass turbofan—are selected as case studies to discuss heat load values in engine bearings, the accessory gearbox, and the power gearbox. The sensitivity of heat load values to engine thrust is also examined to illustrate the correlation between these parameters. Generally, increasing the thrust leads to higher heat loads. However, the heat loads of accessories show minimal sensitivity to thrust changes. In contrast, the sensitivity of heat loads for bearings and the AGB significantly increases. This should be taken into account in the TMS design and development steps as well as in the definition of degradation management strategies. Additionally, a preliminary sensitivity analysis of the effects of the coolant flow rate on engine component temperatures is included. The results highlight the importance of accurate thermal management monitoring systems in next-generation propulsion systems, particularly for the power gearbox in geared turbofan engines, as well as the need for optimal thermal design of the accessory gearbox to reduce its sensitivity to the coolant flow rate.

Author Contributions: Conceptualization, S.J. and A.E.; methodology, A.E. and S.J.; software, S.J., A.E. and T.N.; validation, A.E. and S.J.; formal analysis, A.E. and S.J.; investigation, A.E.; resources, S.J.; writing—original draft preparation, A.E.; writing—review and editing, A.E., S.J. and T.N.; supervision, S.J. and T.N.; project administration, S.J. and T.N. All authors have read and agreed to the published version of the manuscript.

Funding: This research received no external funding.

Institutional Review Board Statement: Not applicable.

Informed Consent Statement: Not applicable.

Data Availability Statement: The data that support the findings of this study are available from the corresponding author upon reasonable request.

Conflicts of Interest: The authors declare no conflicts of interest.

Nomenclature

Symbol	Unit	Meaning
A_i	m^2	Immersion surface area
AOHE		Air Oil Heat Exchanger
b	m	Tooth face width
d	mm	Bearing bore diameter
D	m	Diameter of the rotating element
D_1	inch	Bearing bore diameter
D_2	inch	Outside diameter
D_I	m	Planet bearing bore diameter
d_i	m	Shaft diameter
d_m	mm	Pitch circle diameter
f	-	Friction coefficient
f_0	-	Bearing coefficient of loss
F_A	N	Axial load
fe	-	External mesh coefficient of friction
FOHE		Fuel Oil Heat Exchanger
F_r	-	Froude number
F_R	N	Radial load
h	m	Immersion depth
HEX		Heat exchanger
H_v	-	Gear loss factor
M	N.mm	Friction moment
M_0	Nm	No-load torque planet bearing
M_e	-	External mesh mechanical advantage
n	rpm	Shaft rotational speed
n_B	rpm	Planet bearing rotational speed
P	N	Load of the bearing
P_{BL}	kW	Bearing power loss
P_{in}	kW	Power input
PL_B	kW	Power loss in bearings
PL_{B0}	kW	Bearing churning loss
PL_G	kW	Power loss in meshing gear
PL_{G0}	kW	Gear churning power loss
P_{MLE}	kW	Friction power loss at the sun/planet mesh
P_{MLI}	kW	Friction power loss at the planet/ring mesh
P_{Seal}	kW	Seals churning loss
P_w	kW	Power loss due to windage
Q	kW	Thermal load
Re	-	Reynolds number
t	m	Disk thickness
TBL	Nm	Torque loss per bearing
TP	Nm	Planet gear torque
V_{oil}	m^3	Oil volume
W	lb	Equivalent total load
β_e	degree	Sun/planet angle
ϑ	mm^2/s	Operating viscosity
μ	-	Friction coefficient
μ	Pa s	Lubricant dynamic viscosity
μ_m	-	Mean friction coefficient
ν	m^2/s	Lubricant kinematic viscosity
ρ	kg/m^3	Lubricant density
ω	inch	Bearing width
Ω	rad/s	Rotational speed

References

1. Jafari, S.; Nikolaidis, T. Thermal Management Systems for Civil Aircraft Engines: Review, Challenges and Exploring the Future. *Appl. Sci.* **2018**, *8*, 2044. [CrossRef]
2. Chapman, J.W.; Hasseeb, H.; Schnulo, S. Thermal management system design for electrified aircraft propulsion concepts. In Proceedings of the AIAA Propulsion and Energy 2020 Forum, New Orleans, LA, USA, 26–28 August 2020; pp. 1–23. [CrossRef]
3. Kennedy, D.; Bellamy, O.; Combes, B.; Corner, E.; Pittini, M.; Smith, S.; Stern, J. Meeting the UK Aviation Target-Options for Reducing Emissions to 2050 Committee on Climate Change. 2009. Available online: www.theccc.org.uk (accessed on 30 July 2022).
4. Directorate-General for Mobility and Transport (European Commission); Directorate-General for Research and Innovation (European Commission). *Flightpath 2050: Europe's Vision for Aviation: Maintaining Global Leadership and Serving Society's Needs*; Publications Office: Luxembourg, 2011. [CrossRef]
5. van Heerden, A.S.J.; Judt, D.M.; Jafari, S.; Lawson, C.P.; Nikolaidis, T.; Bosak, D. Aircraft thermal management: Practices, technology, system architectures, future challenges, and opportunities. *Prog. Aerosp. Sci.* **2022**, *128*, 100767. [CrossRef]
6. Srinath, A.N.; Pena López, Á.; Miran Fashandi, S.A.; Lechat, S.; di Legge, G.; Nabavi, S.A.; Nikolaidis, T.; Jafari, S. Thermal Management System Architecture for Hydrogen-Powered Propulsion Technologies: Practices, Thematic Clusters, System Architectures, Future Challenges, and Opportunities. *Energies* **2022**, *15*, 304. [CrossRef]
7. Corchero, G.; Montañés, J.L. An approach to the use of hydrogen for commercial aircraft engines. *Proc. Inst. Mech. Eng. Part G J. Aerosp. Eng.* **2005**, *219*, 35–44. [CrossRef]
8. Donovan, A.; Roberts, R.A.; Wolff, M. Enhanced ECS/Generator Models in an Integrated Air Vehicle Platform. In Proceedings of the 14th International Energy Conversion Engineering Conference, Salt Lake City, UT, USA, 25–27 July 2016; American Institute of Aeronautics and Astronautics: Reston, VA, USA, 2016. [CrossRef]
9. Lents, C.; Hardin, L.; Rheaume, J.; Kohlman, L. Parallel hybrid gas-electric geared turbofan engine conceptual design and benefits analysis. In Proceedings of the 52nd AIAA/SAE/ASEE Joint Propulsion Conference, Salt Lake City, UT, USA, 25–27 July 2016. [CrossRef]
10. Nikolaidis, T.; Jafari, S.; Bosak, D.; Pilidis, P. Exchange Rate Analysis for Ultra High Bypass Ratio Geared Turbofan Engines. *Appl. Sci.* **2020**, *10*, 7945. [CrossRef]
11. Hudson, W.A.; Levin, M.L.; Hudson, W.A.; Levin, M.L. *Integrated Aircraft Fuel Thermal Management*; SAE Technical Papers; SAE International: Warrendale, PA, USA, 1986. [CrossRef]
12. Capitao; Xisto, C.; Jonsson, I.; Lundbladh, A. ENABLEH2 D2.4-Final Report on Heat Management System Deliverable Lead Beneficiary: GKN. Available online: https://ec.europa.eu/research/participants/documents/downloadPublic?documentIds=080166e5f6b47829&appId=PPGMS (accessed on 6 May 2024).
13. Scopus Preview-Scopus-Welcome to Scopus. Available online: https://www.scopus.com/home.uri (accessed on 2 May 2024).
14. Pal, D.; Severson, M. Liquid cooled system for aircraft power electronics cooling. In Proceedings of the 16th InterSociety Conference on Thermal and Thermomechanical Phenomena in Electronic Systems (ITherm), Orlando, FL, USA, 30 May–2 June 2017; pp. 800–805. [CrossRef]
15. Enable H2, Heat Management System Conceptual Design Tools Report ENABLEH2 PUBLIC REPORT ENABLing cryogEnic Hydrogen-Based CO_2-Free Air Transport Deliverable 2.1. Available online: https://ec.europa.eu/research/participants/documents/downloadPublic?documentIds=080166e5eb3948d6&appId=PPGMS (accessed on 6 May 2024).
16. Prashanth, P.; Speth, R.L.; Eastham, S.D.; Sabnis, J.S.; Barrett, S.R.H. Post-combustion emissions control in aero-gas turbine engines. *Energy Environ. Sci.* **2021**, *14*, 916–930. [CrossRef]
17. Jafari, S.; Nikolaidis, T.; Van Heerden, A.S.J.; Lawson, C.P.; Bosak, D. Physics-Based Thermal Model for Power Gearboxes in Geared Turbofan Engines. In Proceedings of the ASME Turbo Expo 2020: Turbomachinery Technical Conference and Exposition, Virtual, 21–25 September 2020; Volume 1. [CrossRef]
18. Jafari, S.; Nikolaidis, T.; Sureddi, R. Physics-Based Thermal Management System Components Design for All-Electric Propulsion Systems. In Proceedings of the ASME Turbo Expo 2021: Turbomachinery Technical Conference and Exposition, Virtual, 7–11 June 2021; Volume 5B. [CrossRef]
19. Jafari, S.; Bouchareb, A.; Nikolaidis, T. Thermal Performance Evaluation in Gas Turbine Aero Engines Accessory Gearbox. *Int. J. Turbomach. Propuls. Power* **2020**, *5*, 21. [CrossRef]
20. Martins, R.C.; Cardoso, N.F.R.; Bock, H.; Igartua, A.; Seabra, J.H.O. Power loss performance of high pressure nitrided steel gears. *Tribol. Int.* **2009**, *42*, 1807–1815. [CrossRef]
21. Palmgren, A. *Ball and Roller Bearing Engineering*; S.H. Burbank & Company, Incorporated: Burbank, CA, USA, 1959.
22. Eschmann, P.; Brändlein, J.; Hasbargen, L.; Weigand, K.; Brändlein, J.; Hasbargen, L.; Weigand, K. *Ball and Roller Bearings—Theory, Design and Applications*; Wiley: Hoboken, NJ, USA, 1999; 492p.
23. Friction and Temperature Rise. Available online: https://www.ntnglobal.com/en/products/catalog/pdf/2203E_a10.pdf (accessed on 18 June 2023).
24. Estimating Bearing Operating Temperature | SKF. Available online: https://www.skf.com/group/products/rolling-bearings/principles-of-rolling-bearing-selection/bearing-selection-process/operating-temperature-and-speed/estimating-bearing-operating-temperature (accessed on 20 May 2023).
25. Harris, T.A.; Kotzalas, M.N. *Essential Concepts of Bearing Technology*; CRC Press: Boca Raton, FL, USA, 2006. [CrossRef]

26. Adams, M.L. *Bearings: Basic Concepts and Design Applications*; CRC Press: Boca Raton, FL, USA, 2018. [CrossRef]
27. Streifinger, H. Fuel/Oil System Thermal Management in Aircraft Turbine Engines. In Proceedings of the RTO Meeting Proceedings, Symposium, Design Principles and Methods for Aircraft Gas Turbine Engines, Toulouse, France, 11–15 May 1998; NATO, 1999. p. 12. Available online: https://apps.dtic.mil/sti/tr/pdf/ADA361702.pdf (accessed on 17 May 2022).
28. Press Releases | Rolls-Royce-Rolls-Royce UltraFan Power Gearbox Tops World Aerospace Record. Available online: https://www.rolls-royce.com/media/press-releases/2021/31-08-2021-rr-ultrafan-power-gearbox-tops-world-aerospace-record.aspx (accessed on 28 March 2023).
29. Autiero, M.; Cirelli, M.; Paoli, G.; Valentini, P.P. A Data-Driven Approach to Estimate the Power Loss and Thermal Behaviour of Cylindrical Gearboxes under Transient Operating Conditions. *Lubricants* **2023**, *11*, 303. [CrossRef]
30. Handschuh, R.U.S. Army, Experimental Study of the Influence of Speed and Load on Thermal Behavior of High-Speed Helical Gear Trains. 2005. Available online: https://ntrs.nasa.gov/citations/20050207440 (accessed on 17 June 2023).
31. Neurouth, A.; Changenet, C.; Ville, F.; Burnet, C.; Octrue, M. Influence of Ball Bearings Modeling on the Predicted Thermal Behavior of a High-speed Gear Unit. In Proceedings of the STLE 70th Annual Meeting & Exhibition, Dallas, TX, USA, 17–21 May 2015.